Functional Materials 15, No.4 (2008)

Volume defects of crystal structure in alkali halide crystals grown from melt by continuous automated method

V.I.Goriletsky, M.M.Tymoshenko, V.V.Vasyliev, T.O. Ilyashenko*

Institute for Scintillation Materials, STC "Institute for Single Crystals", National Academy of Sciences of Ukraine, 60 Lenin Ave., 61001 Kharkiv, Ukraine
*National Technical University "Kharkiv Polytechnical Institute", 21 Frunze St., 61002 Kharkiv, Ukraine

Received August 19, 2008

The types of crystal structure defects (CSD) and the formation causes thereof in CsI(Na), CsI(Tl), and NaI(Tl) crystals of 290 to 520 mm diameter are considered. It has been shown that the CSD of impurity capture type are formed mainly due to disturbed crystallization equilibrium caused by a sharp change in the heat transfer from the growing crystal to water-cooled growth furnace walls. In the ROST units of two generations differing in size and thus in the growing crystal dimensions, this occurs at the height of the crystal cylindrical part of 50 and 70 mm, respectively. The CSD in the form of a local deterioration of the crystal transparence can arise at any crystal height after its exit from the crucible. Those are due to local changes in the crystallization front (CF) shape caused by the temperature variation rate of the controlling heater exceeding the permissible one. This process is accompanied by the crystal diameter increase and acceleration of the crystal linear growth at the CF.

Рассматриваются виды дефектов кристаллической структуры (ДКС) и причины их образования в сцинтилляционных кристаллах CsI(Na), CsI(Tl) и NaI(Tl) диаметром от 290 до 520 мм. Показано, что основной причиной образования ДКС типа захватов посторонних примесей является нарушение условий равновесной кристаллизации, обусловленное резким изменением теплопереноса от растущего кристалла к водоохлаждаемым стенкам ростовой печи. Для установок серии "РОСТ" двух поколений, отличающихся габаритами и, соответственно, размерами выращиваемых кристаллов, это происходит на высоте цилиндрической части кристалла 50 и 70 мм, соответственно. ДКС в виде локального ухудшения прозрачности кристалла могут образовываться на любой высоте кристалла после выхода его из тигля. Причиной их образования является локальное изменение формы фронта кристаллизации (ФК), обусловленное превышением допустимой скорости изменения температуры на регулирующем нагревателе. Этот процесс сопровождается приращением диаметра кристалла и увеличением линейной скорости роста на ФК.

At present, the ROST units provide the growing of large crystals of up to 500 mm diameter at the required quality free of structure defects affecting the scintillation characteristics. However, the fraction of such crystals is still less than 100 % in the mass production. The real value is rather high for the industrial scale and is ensured under the strict maintenance of technical regulations, however, the attained yield of valid production must be considered to be far from the highest limit. The purpose of this work is to study the composition and morphology of CSDs as well as to find a

Table. Impurity content in "special purity (m) 1" NaI produced by TEKHNOIOD

Impurity	Specification requirements (TU 04836770-09-2002) wt.%, at most	Analysis results, wt. %, at most	Impurity	Specification requirements (TU 04836770-09-2002) wt.%, at most	Analysis results, wt. %, at most
H_2O	$2\cdot10^{-1}$	$1\cdot10^{-1}$	Ca	$1\cdot10^{-4}$	$5\cdot10^{-5}$
IO_3^-	$5\cdot10^{-4}$	$44\cdot10^{-4}$	Ba	$5\cdot10^{-4}$	$2\cdot10^{-4}$
OH^-	$5\cdot10^{-4}$	$3\cdot10^{-4}$	Al	$2\cdot10^{-5}$	$1\cdot10^{-5}$
Cl^-	$5\cdot10^{-4}$	$3\cdot10^{-4}$	Fe	$4\cdot10^{-5}$	$3\cdot10^{-5}$
SO_4^-	$5\cdot10^{-4}$	$4\cdot10^{-4}$	Mn	$2\cdot10^{-6}$	$1\cdot10^{-6}$
N	$1\cdot10^{-3}$	$1\cdot10^{-3}$	Cu	$5\cdot10^{-6}$	$4\cdot10^{-6}$
K	$5\cdot10^{-4}$	$5\cdot10^{-4}$	Mo	$2\cdot10^{-5}$	$1\cdot10^{-5}$
Rb	$1\cdot10^{-5}$	$1\cdot10^{-5}$	Tl	$6\cdot10^{-5}$	$4\cdot10^{-5}$
Cs	$5\cdot10^{-6}$	$5\cdot10^{-6}$	Cr	$1\cdot10^{-5}$	$1\cdot10^{-5}$
Mg	$5\cdot10^{-5}$	$3\cdot10^{-5}$	Ti	$7\cdot10^{-5}$	$4\cdot10^{-5}$

correlation between the formation conditions thereof and variations in main technology parameters.

The use of high purity (special purity grade) initial materials excludes the probability of impurity accumulations at grain boundaries in amounts causing the crystal transparence deterioration. Consideration of analytical results for a randomly selected raw material batch shows that it satisfies the specification requirements or even exceeds those in essentially all figures (see Table).

The chemical composition of grown crystals may vary only due to disturbance in the growth process.

The provision of a growing large crystal by raw material at the automated growing in a ROST unit has a specific feature consisting in preparation of a portion of the initial salt at daily demand of 20 to 90 kg (per unit, depending on the crystal to be grown). Therefore, it is unnecessary to prepare up to 0.5 ton of raw material for the whole experiment, thus, the technical problem is simplified considerably. The requirements to the initial salt include, in addition to the specified impurity limits, a low moisture content (less than $1\cdot10^{-3}$ wt.%) and a sufficient looseness necessary for satisfactory operation of the vibrational scale. Those requirements are realized as a rule by the raw material deep de-watering. The water removal realized by heating in vacuum may cause the raw material contamination with its hydrolysis products (CO_3^{2-}, OH^-), if the heating rate exceeds that of water evaporation (the adsorbed water is known to be removed in vacuum only at a slow heating of the salt [1]). In other words, a large crystal can be grown without any deviations from the growing process but areas with inhomogeneous internal structure can be revealed therein due, e.g., to a high CO_3^{2-} ion concentration in the growing crystal.

A technique has been developed [2] and being used at present that provides the burning-out of organic compounds directly in the salt. It is, however, an additional contamination source both by the hydrolysis products and by impurities present in the dry air.

Taking into account the above technological factors, two CSD types are expected to be formed. First of all, those are local areas with included impurity phase. Those may be of 1 to 100 mm in size and are visible well with the naked eye. Such defects are able to change the preset crystallographic orientation of the crystal in their areas and cause polycrystalline formations. As the final result, a considerable part of the crystal or even the whole large crystal becomes useless due to such CSDs. Second, a CSD can take the form of a local deteriorated transparence area of several millimeters in size. Those are revealed most often visually and more seldom at the transparence measurements on samples taken from the crystal. Both CSD types form non-scintillating areas in the final produced modules and thus are inadmissible.

An extremely rare CSD example in AHC is shown in Fig. 1. When considering that crystal through a cut along the growth axis

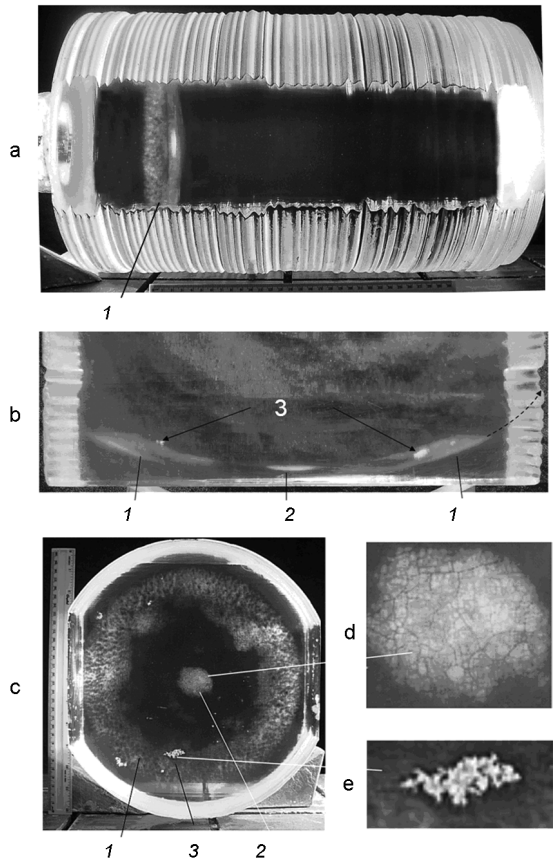

Fig. 1. A large CsI(Na) single crystal with volume CSD in the upper part (a) and its fragments cut along (b) and across (c) the growth axis as well as microphotos of a disc (d) and dendrite (e).

(with illumination through the seed), complex foreign inclusions are observed at the CF shaped as a ring with a disc in the middle part (Fig. 1a). The details of the defect are presented in the fragments of that crystal cut in parallel (Fig. 1b) and perpendicular (Fig. 1c) to the ingot axis as well as in magnified fragments (Figs. 1d, 1e). In all the photos, the CF is seen to loss its stability while in microphotos the grain boundaries of the quenched melt are seen. The dendrites evidence clearly that the CF has lost its smooth shape that is possible at an excessive overcooling of the melt. The electron microscopy of a cleaved fragment of that crystal revealed also the foreign phase inclusions among which the activator phase predominates.

The bottom heater temperature (t_{bot}) variation during the whole growing cycle is characterized by a monotonous temperature decrease followed by a minimum ($t_{bot,min}$) corresponding to the time point when the crystal upper butt leaves the crucible upper

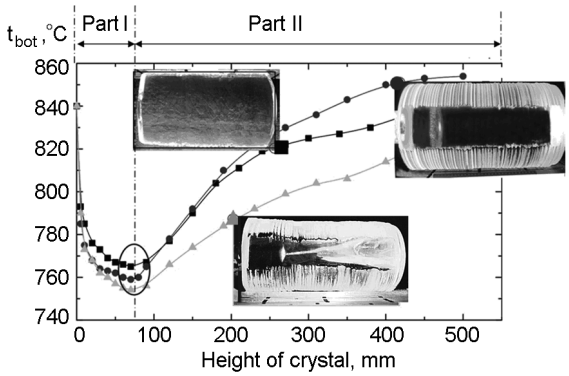

Fig. 2. Temperature dynamics of automated t_{bot} correction as a function of the CsI(Na) crystal length. The dashed line separates two heat exchange phases during the growing.

edge. Then the heat transfer from the crystal starts to rise and thus the automatic control system (ACS) provides the t_{bot} elevation. The real t_{bot} position varies from one experiment to another and depends on numerous parameters that define the dynamics of the growth process itself. In fact, it is seen in Fig. 2 that the t_{bot} vector changes to the opposite one in that point. Consideration of the ACS operation shows that in the specific time point of the heat transfer jump, the system functions do not provide the timely situation estimation and thus the correcting control lags. This is caused by the fact that the ACS measures the crystal diameter and corrects the temperature only several times over an hour [3]. This seems to be insufficient to reveal galloping events and all the more to prevent the consequences thereof. The equilibrium crystallization in that time point can be provided only by fast action of the ACS enable of readjusting its control functions in the opposite direction without any backlash. Fig. 2 shows that the absolute $t_{bot,min}$ values are different in three experiments (♦, 765; •, 759; ■, 754°C) and only the crystal with the highest $t_{bot,min}$ is free of CSDs.

The geometric coordinate of the CSD position in the crystal corresponds to $t_{bot,min}$ and to the cylindrical part height of 50 mm for the first generation units and 70 mm for the second one. It is seen in Fig. 2 (two lower CsI(Na) of 290 mm in dia. with longitudinal cuts) the equilibrium crystallization conditions were distorted with a foreign phase inclusion at the cylindrical part height (H_{cr})≈50 mm (just at that height the $t_{bot,min}$ took place). Although those events were short-term and followed by an increase

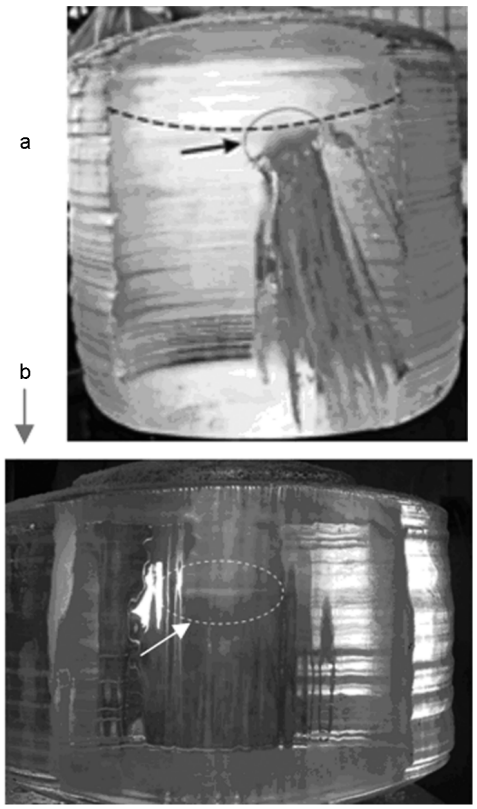

Fig. 3. Formation of crystal structure defects (shown by arrows) in the middle of the crystallization front (the CF calculated shape shown by dashed line) in the growing course of a CsI(Tl) crystal 450 mm in dia. (a) and a NaI(Tl) one 500 mm in dia. (b).

in t_{bot}, the crystal defect part is unsuitable for scintillation devices.

A similar situation is observed also in CsI(Tl) crystals of a larger diameter. This is seen in Fig. 3 that presents a longitudinal cut of a 450 mm diameter ingot. At a height of about 60–70 mm, CSDs of the impurity capture type are seen giving rise to polycrystalline boundaries. It is very difficult to make a similar image for a NaI(Tl) single crystal because it is highly hygroscopic. To that end, the crystal should be wetted simultaneously at both sides, but the shot is not always possible due to the cut instantaneous blooming or the ingot cracking. A successful attempt is shown in Fig. 3b where the impurity capture is seen at the center of a 500 mm diameter NaI(Tl) crystal.

The above described trend in the temperature variation of the controlling heater is the same for CsI(Na), CsI(Tl) and NaI(Tl) and is defioned by the temperature field features and crucible design of the ROST unit. Thus, the regularities of CSDs formation are identical, too. The melt has sufficient time to be overcooled due to increasing heat transfer from the crystal that has its upper butt already in the zone of direct heat radiation to the water-cooled furnace walls. The temperature correction formed by the ACS has a lag relative to the process onset, thus, the defect thickness at the CF (being defined by the duration and value of the overcooling near the CF) can be different (2 to 7 mm).

To check this statement, a special experiment was carried out (see Fig. 4) where the t_{bot} was varied intentionally after the crystal butt was higher than the crucible upper edge. The intervention time points are shown at the left side of chart strip as numbered circles as well at the crystal (right figure side) by numbers. It follows from the Figure that the formation of impurity inclusions initiated by the t_{bot} decrease is mani-

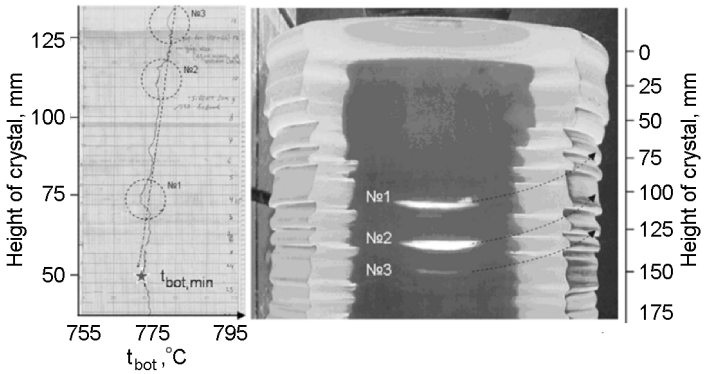

Fig. 4. A fragment of operation diagram and photo of the crystal defect area. The defects in CF and the t_{bot} changes corresponding thereto are denoted by numbers. The calculated CF is shown by dashed line. The asterisk indicates $t_{bot,min}$.

fested itself in the CF middle part. If the calculated CF shape (dashed line) is superimposed onto the Figure, all the three defect areas are seen to correspond to increase of the crystal diameter. Let the diagram be considered in more details, starting from below (in the crystal growth direction). In the crystal part corresponding to $t_{bot,min}$ (H_{cr}≈50 mm), no defects are formed, that is, the ACS has already managed the situation. As the crystal was grown above the crucible edge H_{cr} ≈75 mm, the first intervention was done, the t_{bot} being decreased by 3°C at a rate of 6°C/h followed by 25 min holding and increase by the same value but at a lower rate (3°C/h). As a result, the area No.1 about 6 mm in height has been formed in the crystal with the impurity capture. The next step, at H_{cr}≈100 mm, consisted in the t_{bot} decrease by 1.5°C at a rate of 3°C/h followed by 45 min holding and t_{bot} increase by 4°C at a rate of 8°C/h. The defect area (No.2) is 7–8 mm thick in that case. The third intentional intervention was done at H_{cr} = 125 mm by decreasing t_{bot} by the same value at the same rate, 5 min holding and re-increasing by the above-mentioned value at the above-mentioned rate. The intervention trace (area No.3) in the crystal is about 1–2 mm thick.

Thus, by simulating various melt overcooling degrees relative to its equilibrium state for specific moments of the crystal growth, we have obtained a correlation between the melt overcooling duration and the crystal defect area size.

It has been noted above that the volume defects in a crystal arise in connection with the profile of its side surface. In all the defect zones, the crystal diameter is increased in most cases. If we have started from the study of the diameter variations, the defects at the CF were found in the zones where the diameter increase rate exceeded the critical value. At the other hand, the crystal side surface profile is connected directly to the controlled parameter t_{bot}. Continuing these considerations, we conclude again that the ACS plays a part in the CSDs formation.

Let the growth be considered from the viewpoint of physical processes. As to heat transfer, the growth process can be subdivided into two steps (see Fig. 2). The first one is accompanied by t_{bot} decrease, while t_{bot} being increasing intensely in the second step. During the first step, the automated control process never caused volume CSDs

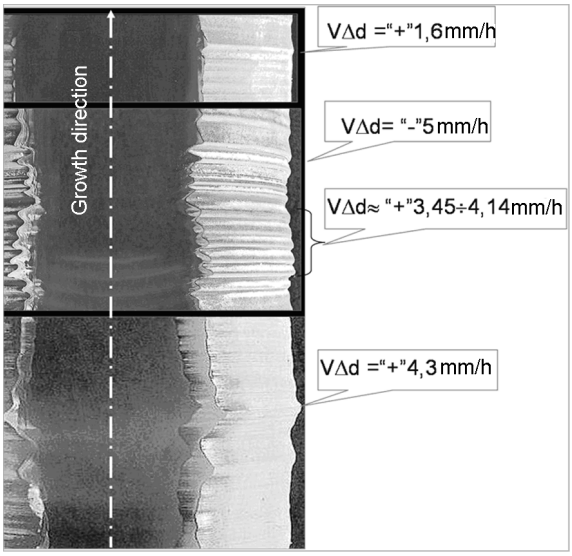

Fig. 5. Fragments of longitudinal cross-section of crystals having diameter changes with various increment rates. The footnotes indicate such areas on the crystal side surface and the diameter increment rates.

formation in any AHC. This is due to the fact that to maintain the dynamic equilibrium of crystallization, the melt temperature at any time point should be lower than the crystallization one by a specified value. In this growth step, the crystal is unable to remove heat towards the water-cooled furnace wall due to its geometric position relative to the crucible as well as to the presence of a condensate layer on its surface. That is why the ACS causes the t_{bot} decrease. In other words, the crystal growth should be initiated in each subsequent time point by decreasing the melt temperature, otherwise, the crystal growth stops. Thus, if the ACS will not provide a recurrent decrease of t_{bot} due to erroneous signal from the melt level sensor, this will not result in a CSD formation but only in the crystallization slowdown or stop.

In the second process step, the situation is quite opposite. Here, the crystal growth should be stopped in each subsequent time point, because the crystal is within the active heat removal zone due to the ingot constant cooling. In this case, only the furnace atmosphere is present between the crystal and the water-cooled furnace wall, thus, the heat exchange is unhindered. In addition, the crystal side surface is coated with a thinner condensate layer than its butt, thus enhancing the heat removal from the ingot. Therefore, if the ACS will not provide a sufficient t_{bot} increase due to erroneous information from the melt level sensor or,

even worse, will provide a decrease thereof, this may cause a critical overcooling of the melt followed by formation of a CSD as a local transparence change in the crystal volume (see Fig. 5). The CSD size and density are defined by the crystal diameter increase rate or, in more correct words, the change rate of t_{bot}. It follows from experimental data, that no CSDs are observed at the crystal diameter increase rate of 1.6 mm/h (the expansion at the crystal upper fragment in Fig. 5). The crystal diameter diminution at any rate does not affect the crystal, while a series of alternating diameter changes (the lower part of middle fragment in Fig. 5) where the diameter increment rate was 3.45 to 4.14 mm/h has resulted in a series of impurity captures visible as stripes in the crystal similar to the growth stripes in semiconductors and other crystals [4]. The lower fragment of Fig. 5 shows the formation of an extended ingot area with deteriorated transparence caused by the crystal diameter increase at a rate of about 4.4 mm/h.

By comparing these and other data on the crystal diameter increase rate and the t_{bot} change rates corresponding thereto, the maximum allowable crystal diameter deviations at the automated correction of t_{bot} parameter.

To conclude, the CSDs of the impurity capturing type are caused by distortion of the crystallization equilibrium due to a sharp change in the heat transfer from the growing crystal to the water-cooled walls of the growth furnace at the crystal cylindrical part height of 50 to 70 mm. The local transparence deterioration may arise at any crystal height due to exceeding of the allowable temperature change rate of the controlling heater. This process is always accompanied by the crystal diameter increment and increased linear growth speed at the CF. The crystal diameter increase rate should not exceed 2 mm/h, while the allowable temperature decrease rate of the bottom heater is maximum 1°C/h.

References

1. N.N.Smirnov, Phil. Dr.Thesis, Institute for Single Crystals, National Academy of Sciences of Ukraine (1996).
2. Russian Fed. Pat. 1039253, Cl.C 30 B29/12, C 30 B (publ. 1993).
3. S.K.Bondarenko, V.I.Goriletsky, V.S.Susdal, *Functional Materials*, **6**, 380 (1999).
4. G.Mueller, *J. Cryst. Growth*, **35** , 138 (1991).

Об'ємні дефекти кристалічної структури лужно-галоїдних кристалів, що вирощені з розплаву безперервним автоматизованим методом

В.І.Горілецький, М.М.Тимошенко, В.В.Васильєв, Т.О.Ільяшенко

Розглядаються типи дефектів кристалічної структури (ДКС) та причини їх утворення у сцинтиляційних кристалах CsI(Na), CsI(Tl) та NaI(Tl) діаметром від 290 до 520 мм. Показано, що головною причиною утворення ДКС типу захоплень сторонніх домішок є порушення умов рівноважної кристалізації, що спричиняється різкою зміною теплоперенесення від кристала, що росте, до стінок вирощувальної печі, що водоохолоджуються. Для установок серії "РОСТ" двох поколінь, що відрізняються габаритами і, відповідно, розмірами кристалів, що ростуть, це відбувається на висоті циліндричної частини кристала відповідно 50 та 70 мм. ДКС у вигляді локального погіршення прозорості кристала можуть утворюватися на будь-якій висоті кристала після його виходу з тигля. Причиною їх утворення є локальна зміна форми фронту кристалізації (ФК), зумовлене перевищенням граничної швидкості зміни температури на нагрівачі, що регулюється. Цей процес супроводжується приростенням діаметра кристала та збільшенням лінійної швидкості росту на ФК.